Environmental Science & Technology

Article

Cite This: Environ. Sci. Technol. 2018, 52, 8381−8389

pubs.acs.org/est

Influence of Particle Physical State on the Uptake of Medium-Sized Organic Molecules

Zhaoheng Gong,[†] Yuemei Han,[†] Pengfei Liu,[†] Jianhuai Ye,[†] Frank N. Keutsch,[†,‡] Karena A. McKinney,[†,∥] and Scot T. Martin*[,†,§]

[†]John A. Paulson School of Engineering and Applied Sciences, Harvard University, Cambridge, Massachusetts 02138, United States

[‡]Department of Chemistry and Chemical Biology, Harvard University, Cambridge, Massachusetts 02138, United States

[§]Department of Earth and Planetary Sciences, Harvard University, Cambridge, Massachusetts 02138, United States

Supporting Information

ABSTRACT: The uptake of medium-sized levoglucosan and 2,4-dinitrophenol to organic particles produced by α-pinene ozonolysis and to ammonium sulfate particles was studied from 10% to >95% relative humidity (RH). For aqueous sulfate particles, the water-normalized gas-particle partitioning coefficient of levoglucosan decreased from $(1.0 \pm 0.1) \times 10^{-3}$ to $(0.2 \pm 0.1) \times 10^{-3}$ $(\text{ng } \mu\text{g}^{-1})_{\text{particle}}/(\text{ng m}^{-3})_{\text{gas}}$ from 40% to >95% RH, suggestive of a salting-in mechanism between levoglucosan and ionic ammonium sulfate solutions. For the organic particles, the levoglucosan partitioning coefficient increased from 10% to 40% RH and became invariant at $(2.0 \pm 0.4) \times 10^{-3}$ $(\text{ng } \mu\text{g}^{-1})/(\text{ng m}^{-3})$ above 40% RH. A kinetic limitation on uptake below 40% RH was implied, compared to a thermodynamic regime above 40% RH. The estimated diffusivity was $10^{-19\pm0.05}$ $\text{m}^2\ \text{s}^{-1}$ at 40% RH. By comparison, the uptake of 2,4-dinitrophenol onto the organic particles was below detection limit, implying an upper limit on the partitioning coefficient of 6.8×10^{-6} $(\text{ng } \mu\text{g}^{-1})/(\text{ng m}^{-3})$ at 80% RH. The results highlight that the molecular uptake of gases onto particles can be regulated by both kinetic and thermodynamic factors, either of which can limit the uptake of medium-sized organic molecules by atmospherically relevant particles.

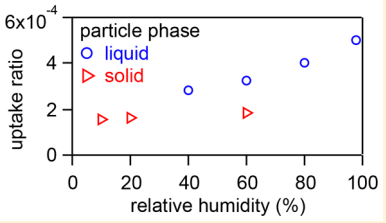

1. INTRODUCTION

Atmospheric particles have important roles in climate[1] and human health.[2] Atmospheric particles can remain suspended for as long as several days to a few weeks as they are advected around Earth, and they can undergo physical and chemical processes during this time that change their properties continuously. Uptake is one process that can significantly influence the composition of both the gas and particle phases. The rate and extent of uptake can be described by kinetic and thermodynamic regimes, respectively. An understanding of the conditions under which each regime dominates is needed for quantitative predictions of uptake under real atmospheric conditions.

Particle physical state is one important property that can significantly influence gas-particle interactions.[3−5] Under atmospheric conditions, particles can be of different physical states, such as liquid, semisolid, and solid. The particle water content and hence physical state can vary with relative humidity (RH), temperature, and chemical composition.[3,4,6,7] Atmospheric salts such as ammonium sulfate have deliquescence and efflorescence points that lead to a bifurcation between solid and liquid physical states. By comparison, atmospheric organic particles are often a mixture of thousands or tens of thousands of compounds,[8] and the viscosity varies smoothly from solid-like to liquid-like across the range of atmospheric RH.[6,9−11]

This continuum in viscosity with changes in atmospheric conditions could suggest transitions between kinetic and thermodynamic regimes for many gas-particle uptake processes.[12,13] Species diffusivity within the particle material is a key determinant of whether a kinetic or a thermodynamic regime prevails. Significant literature has focused on the uptake of small reactive inorganic molecules such as O_3,[14] N_2O_5,[15] HO_2,[16] or NH_3.[17−19] The uptake of medium-sized organic molecules, especially in relation to particle physical state, has received considerably less attention.[20−22] Species diffusivity is a complex quantity linked both to the diffusing species and the host matrix. Typically there is a monotonic relationship between diffusivity of a guest species and viscosity of the host matrix. The exact mathematical forms, however, can follow power laws of different orders and different slopes among species-matrix pairs.[23] For these reasons, the uptake and diffusion of medium-sized organic molecules could differ from predictions based on results obtained for small, inorganic molecules, even within the same type of host matrix.

Phenol, nitrophenol, and levoglucosan constitute examples of medium-sized molecules. They are typical particle-phase tracer molecules used to identify biomass-burning emissions

Received: April 20, 2018
Revised: July 1, 2018
Accepted: July 13, 2018
Published: July 13, 2018

DOI: 10.1021/acs.est.8b02119
Environ. Sci. Technol. 2018, 52, 8381−8389

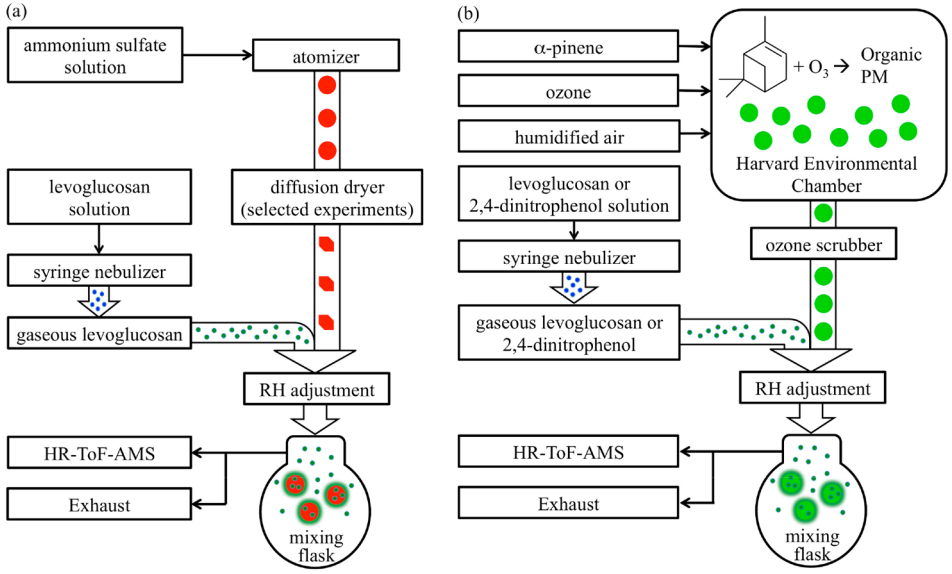

Figure 1. (a) Setup for experiments using ammonium sulfate particles. (b) Setup for experiments using α-pinene-derived organic PM. Abbreviations: PM, particulate matter; HR-ToF-AMS, high-resolution time-of-flight aerosol mass spectrometer.

and transport.[24,25] In addition to their presence in the primary emissions of biomass-burning particles, these species are also released into the gas phase during biomass-burning events and to a lesser extent from urban and industrial sources. The possible uptake of these molecules into types of atmospheric particles other than biomass-burning particles, such as biogenic particulate matter (PM), is of interest, as related to possibly altering the optical properties of those particles.[26] Uptake into biogenic PM could differ from uptake into biomass-burning particles because of different chemistry and properties among the particle types.[27,28] Of further interest, analytical techniques such as aerosol mass spectrometry techniques that do not study single particles could confuse sources if medium-sized analyte molecules can facilely exchange through the gas phase among varied particle types.[29,30]

Herein, two biomass-burning-related organic molecules, levoglucosan and 2,4-dinitrophenol, were used as gas-phase probe molecules to study the effects of particle physical state on the uptake of medium-sized organic molecules. Sulfate and organic PM, two prevalent particle types in urban and rural atmospheres,[31,32] were used as host matrices in the experiments. Three sets of experiments were conducted to study uptake processes: (a) gas-phase levoglucosan and particles of ammonium sulfate, (b) gas-phase levoglucosan and organic PM derived from α-pinene ozonolysis, and (c) gas-phase 2,4-dinitrophenol and organic PM derived from α-pinene ozonolysis. The evolution of uptake with relative humidity was a focus of the study. Thermodynamic and kinetic factors and transitions between thermodynamically and kinetically controlled regimes with relative humidity are discussed.

2. EXPERIMENTAL SECTION

2.1. Aerosol Particle Populations. The experimental setup to study the uptake of levoglucosan onto ammonium sulfate particles is shown in Figure 1a. A population of submicrometer aerosol particles was produced by atomization (model 3076, TSI Inc., Shoreview, MN) of an aqueous solution of ammonium sulfate (≥99.0%, Sigma-Aldrich; 0.1% w/w). The atomizer was operated at a flow rate of 1.5 L min^{-1} of zero air. For some experiments, the flow after the atomizer passed through a diffusion dryer to prepare a population of effloresced solid particles (<35% RH). In other experiments, the dryer was removed, and the particle population remained aqueous. In this way, given efflorescence at 35% RH and deliquescence at 80% RH, the particles were either solid or aqueous depending on RH history (i.e., hysteresis experiments), and comparative uptake experiments were carried out.[3,33] The log-normal number-diameter distribution of the particle population had geometric diameter of 210 ± 20 nm (represented as mean ± one-sigma standard deviation throughout the text) and geometric standard deviation of 100 ± 10 nm. The integrated number concentration was (2.0 ± 0.3) × 10^3 cm^{-3}.

A different experimental setup was employed to study the uptake of levoglucosan and 2,4-dinitrophenol onto a population of organic aerosol particles (Figure 1b). For these experiments, in place of sulfate particles, submicrometer organic particles were produced in the Harvard Environmental Chamber (HEC) by the dark ozonolysis of α-pinene. The log-normal number-diameter distribution of the particle population had a geometric diameter of 200 ± 20 nm and geometric standard deviation of 80 ± 10 nm. The integrated number concentration was (2.6 ± 0.2) × 10^3 cm^{-3}. The chamber and its operation were described previously.[34,35] In brief, the chamber was operated as a continuously mixed flow reactor (CMFR), characterized by a residence time of 4.2 h, a relative humidity of 40 ± 0.1%, and a temperature of 298 ± 1 K. For the levoglucosan uptake experiments, 20 ppb α-pinene (in the absence of reaction) and 300 ppb ozone were used in the HEC. For the 2,4-dinitrophenol uptake experiments, 40 ppb α-pinene and 300 ppb ozone were used. For both cases, α-pinene reacted to completion by ozonolysis, and the particle composition characterized by mass spectrometry (see Section 2.4) was indistinguishable between the two sets of experiments. The outflow from the HEC passed through an annular ozone scrubber before being used in the exposure and uptake experiments. The scrubber reduced ozone concentrations to below the limit of instrument detection (<5 ppb).

2.2. Gas-Phase Probe Molecules. The particle flows mixed with flows of either gas-phase levoglucosan or gas-phase

DOI: 10.1021/acs.est.8b02119
Environ. Sci. Technol. 2018, 52, 8381−8389

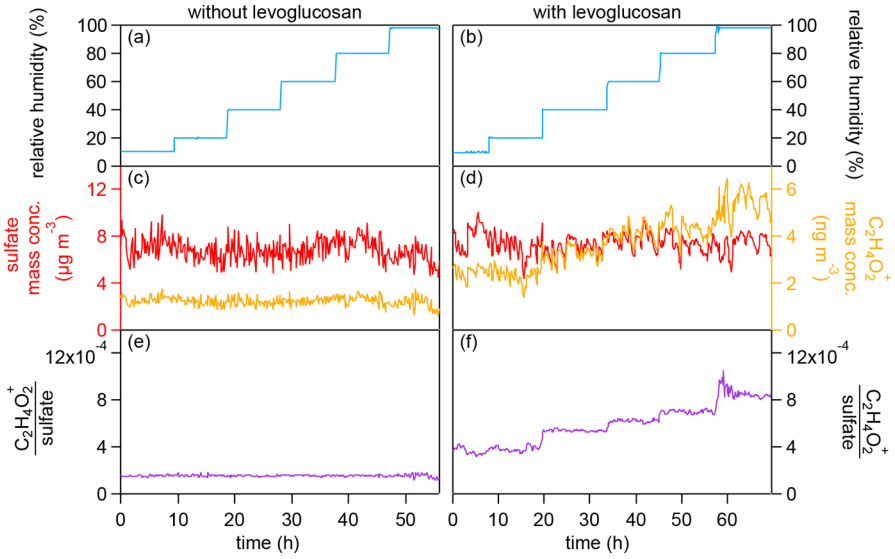

Figure 2. Uptake of levoglucosan ($C_2H_4O_2^+$ ion) by ammonium sulfate particles for variable relative humidity. Measurements were made by an HR-ToF-AMS under the conditions of no levoglucosan (left column) and exposure to 0.20 ppb levoglucosan in the gas phase (right column).

2,4-dinitrophenol for exposure and uptake experiments (see Figure 1a and b). Flows of gas-phase levoglucosan and 2,4-dinitrophenol were produced by a syringe-nebulizer-evaporation system. Aqueous solutions of levoglucosan (≥99.0%, Sigma-Aldrich; 1% w/w) or 2,4-dinitrophenol (≥99.0%, Sigma-Aldrich; 0.2% w/w) were pushed through a nebulizer (Meinhard A3, PerkinElmer Inc., Waltham, MA; zero-air flow rate of 1 L min^{-1}) by a syringe pump (Fusion 200, Chemyx Inc., Stafford, TX; liquid flow rate of 20 μL h^{-1} for levoglucosan and 50 mL h^{-1} for 2,4-dinitrophenol). The nebulized droplets evaporated, leaving the organic molecules in the gas phase at <5% RH. The gas flow and the particle flow combined upstream of a 7-L reaction flask. Based on mass balance with the nebulized solution and subsequent dilution, the calculated levoglucosan concentration inside the flask was 0.20 ppb (1.3 μg m^{-3}), which was below its saturation concentration of 0.47 ppb (3.1 μg m^{-3}).[36] The concentration of 2,4-dinitrophenol was 90 ppb (680 μg m^{-3}) based on mass balance compared to a saturation concentration of 510 ppb (3.8×10^3 μg m^{-3}).[37]

2.3. Exposure and Uptake. The reaction flask served as a CMFR. It was operated at a flow rate of 2.1 L min^{-1}, a residence time of 200 s, and a temperature of 298 K ± 1 K. Relative humidity inside the flask was monitored (Rotronic Sensor, Bassersdorf, Switzerland), and the RH of the combined inflow was adjusted by passage through a Nafion-tube setup (Perma Pure, Lakewood, NJ) just upstream of the flask inlet. In this way, a feedback system controlled RH in the flask to a set point value, which was adjusted from 10% to 90% for different experiments. For RH > 95%, a shallow layer of water was poured into the bottom of the flask prior to the experiments. Uptake of levoglucosan or 2,4-dinitrophenol to the different particle types was determined based on changes in the composition of the particles in the outflow from the reaction flask.

2.4. Analytical Methods. The composition of the particles in the flask outflow was characterized using a high-resolution time-of-flight aerosol mass spectrometer (AMS, Aerodyne Inc., Billerica, MA). For each uptake experiment, background measurements in the absence of levoglucosan or 2,4-dinitrophenol and exposure measurements in their presence were conducted. The AMS was operated in both a high-sensitivity mode ("V-") to quantify uptake and a high-resolution mode ("W-") to better identify ion fragments. Ionization efficiency was calibrated using particles of ammonium nitrate (≥99.0%, Sigma-Aldrich). The AMS software packages *SQUIRREL* (Version 1.55H) and *PIKA* (Version 1.14H) were used for data analysis. The fragmentation tables in *SQUIRREL* and *PIKA* were adjusted for the experimental conditions of the HEC.[38] Mass concentrations were based on the default relative ionization efficiencies of 1.4 and 1.2 for organic and sulfate species, respectively.[39] A particle collection efficiency of unity was used. Ratio quantities used herein, such as $C_2H_4O_2^+$/sulfate, $C_2H_4O_2^+$/organic, and $\sum C_xH_yO_zN_w^+$/organic, were independent of possible variations in the AMS collection efficiency with particle composition, physical state, and relative humidity.

In control experiments in the absence of particles, the gas phase was sampled upstream and downstream of the reaction flask by a proton-transfer-reaction time-of-flight mass spectrometer (PTR-TOF-MS 8000, Ionicon Analytik GmbH, Austria). The upstream and downstream gas-phase concentrations were the same within experimental uncertainty, confirming the absence of signficant wall loss in the apparatus (see Supporting Information (SI), Section S1). The estimated maximum uptake in the presence of particles did not decrease the calculated gas-phase concentrations of levoglucosan and 2,4-dinitrophenol sufficiently for detection within the noise limits of the PTR-TOF-MS, as confirmed by the observations (SI Figure S1).

3. RESULTS

3.1. Uptake of Levoglucosan by Ammonium Sulfate Particles. Results from the uptake experiments of levoglucosan onto ammonium sulfate particles are shown in Figure 2. The ratio $C_2H_4O_2^+$/sulfate is plotted for stepwise increases in RH from 10% to >95%. The ion fragment $C_2H_4O_2^+$ at m/z 60 served as a tracer ion for levoglucosan detection by the AMS.[40] This fragment accounted for 18% of the total AMS signal

DOI: 10.1021/acs.est.8b02119
Environ. Sci. Technol. 2018, 52, 8381−8389

Table 1. Effect of Relative Humidity on the Mass-Normalized Uptake of Levoglucosan by Aerosol Particles of Ammonium Sulfate and α-Pinene-Derived Organic PM. Results Are Plotted in Figure 5

		uptake of levoglucosan onto particles of ammonium sulfate		uptake of levoglucosan onto particles of α-pinene-derived secondary organic material		
RH (%)	phase	$\Delta\left(\frac{C_2H_4O_2^+}{\text{ammonium sulfate}}\right)$	$\Delta\left(\frac{C_2H_4O_2^+}{\text{ammonium sulfate + water}}\right)$	RH (%)	viscosity (Pa s)[56,62]	$\Delta\left(\frac{C_2H_4O_2^+}{\text{organic}}\right)$
10	solid	$(1.5 \pm 0.2) \times 10^{-4}$		10	$10^{8.1\pm0.5}$	$(2.6 \pm 0.8) \times 10^{-4}$
20	solid	$(1.7 \pm 0.2) \times 10^{-4}$		20	$10^{7.7\pm0.5}$	$(3.4 \pm 0.9) \times 10^{-4}$
60	solid[a]	$(1.8 \pm 0.2) \times 10^{-4}$				
40	liquid	$(2.8 \pm 0.1) \times 10^{-4}$	$(2.2 \pm 0.1) \times 10^{-4}$	40	$10^{7.2\pm0.6}$	$(4.6 \pm 0.9) \times 10^{-4}$
60	liquid	$(3.4 \pm 0.1) \times 10^{-4}$	$(2.1 \pm 0.1) \times 10^{-4}$	60	$10^{5.4\pm2.2}$	$(4.8 \pm 0.9) \times 10^{-4}$
80	liquid	$(4.0 \pm 0.2) \times 10^{-4}$	$(1.7 \pm 0.2) \times 10^{-4}$	80	$10^{1.8\pm0.4}$	$(4.9 \pm 0.8) \times 10^{-4}$
				90	$10^{0.8\pm0.4}$	$(5.0 \pm 0.8) \times 10^{-4}$
>95	liquid	$(5.0 \pm 0.2) \times 10^{-4}$	$(0.5 \pm 0.2) \times 10^{-4}$	>95		$(5.1 \pm 0.8) \times 10^{-4}$

[a]Particles were dried below the efflorescence RH before increasing to 60% RH.

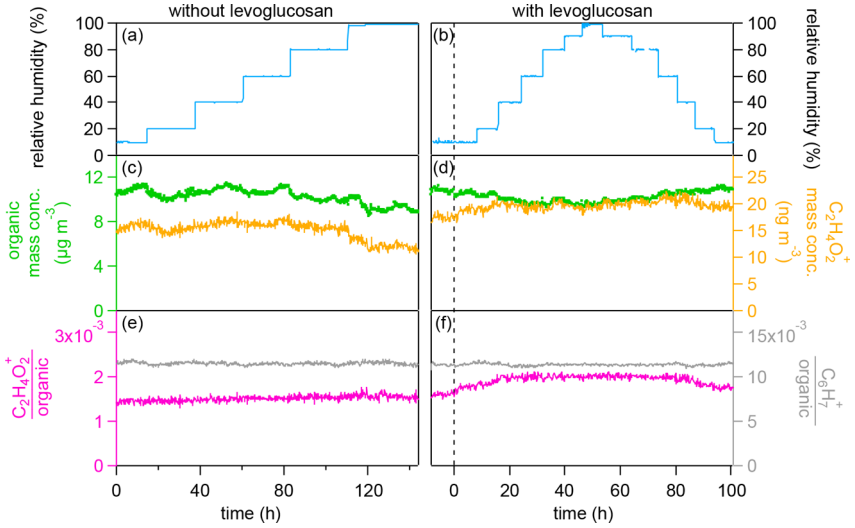

Figure 3. Uptake of levoglucosan ($C_2H_4O_2^+$ ion) by α-pinene-derived organic PM for variable relative humidity. Measurements were made by an HR-ToF-AMS under the conditions of no levoglucosan (left column) and exposure to 0.20 ppb levoglucosan in the gas phase (right column). Results are also shown for a control ion ($C_6H_7^+$), which was a strong ion for α-pinene-derived organic PM and to which levoglucosan did not contribute.

intensity in calibration experiments using pure levoglucosan particles, in agreement with other studies.[41,42]

Panel sets in the left and right columns of Figure 2 show experiments in the absence and presence of gas-phase levoglucosan, respectively. For both sets of experiments, the upper side of the hysteresis loop of ammonium sulfate was represented, meaning that the particles were solid below 35% RH and aqueous above 35% RH. In the absence of levoglucosan, the ratio $C_2H_4O_2^+$/sulfate was $(1.55 \pm 0.09) \times 10^{-4}$, and this ratio was insensitive to changes in RH within experimental sensitivity. This value thus represented a background reference for experiments in the presence of gas-phase levoglucosan. Changes relative to this background value during the experiment were calculated as $\Delta(C_2H_4O_2^+/\text{sulfate})$ and adjusted to $\Delta(C_2H_4O_2^+/\text{ammonium sulfate})$ (Table 1), where ammonium sulfate mass concentration is taken as (132/96) × sulfate concentration. Given uncertainties in ammonium measurement in the AMS,[43] this calculation was considered more accurate. Water content was accounted for by calculation (SI, Section S3), and values of $\Delta(C_2H_4O_2^+/(\text{ammonium sulfate + water})$ are listed in Table 1. For solid particles in the presence of gas-phase levoglucosan, $\Delta(C_2H_4O_2^+/\text{ammonium sulfate})$ increased by $(1.5 \pm 0.2) \times 10^{-4}$ at 10% RH. This increase is believed to represent surface adsorption. For aqueous particles, the ratio $C_2H_4O_2^+$/sulfate increased stepwise with increases in RH, and $\Delta(C_2H_4O_2^+/\text{ammonium sulfate})$ overall tripled from 40% to >95%. A comparative experiment at 60% for solid particles prepared on the lower side of the hysteresis loop had the same ratio $C_2H_4O_2^+$/sulfate as for <35% RH (results not shown; see Table 1).

3.2. Uptake of Levoglucosan by A-Pinene-Derived Organic Particles. Results of levoglucosan uptake experiments on α-pinene-derived organic particles are shown in Figure 3. Experiments were conducted in the absence of levoglucosan (left column) as well as in its presence (right column). Figure 3a and b show the RH profiles. RH was first stepwise increased from 10% to >95%, after which it was stepwise decreased to 10%. The organic PM concentration and the mass-equivalent concentration of the $C_2H_4O_2^+$ ion intensity from the AMS are plotted in Figure 3c and d. The

DOI: 10.1021/acs.est.8b02119
Environ. Sci. Technol. 2018, 52, 8381−8389

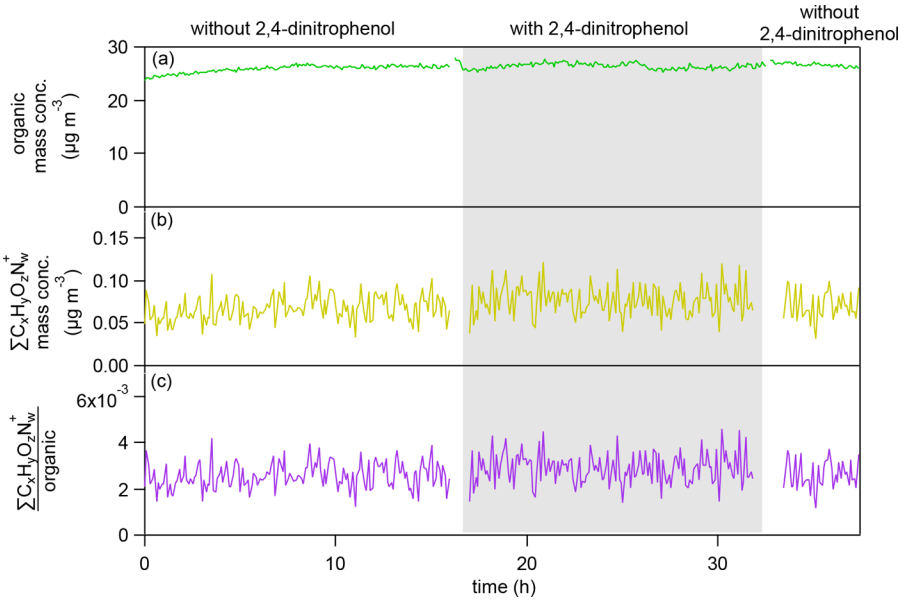

Figure 4. No observable uptake of 2,4-dinitrophenol (represented by the $\Sigma C_xH_yO_zN_w^+$ ion family) by α-pinene-derived organic PM at 80% RH. Experiments were conducted in the absence of 2,4-dinitrophenol (white background) and in the presence of 90 ppb of 2,4-dinitrophenol in the gas phase (shaded background).

ratios $C_2H_4O_2^+$/organic and $C_6H_7^+$/organic, representing respectively the primary observable of the experiment and a corresponding control, are plotted in Figure 3e and f.

In the absence of gas-phase levoglucosan, the ratio $C_2H_4O_2^+$/organic was $(15.1 \pm 0.7) \times 10^{-4}$ (Figured 3e). This value, characteristic of the organic particles, represented a background signal for purposes of the uptake experiment. Figure 3e shows that the background signal was not sensitive to RH within experimental sensitivity from 10% to >95% RH. The background signal differed for the organic experiments compared to the sulfate experiments because of the organic compared to inorganic particle composition between the two sets of experiments. Changes relative to the background signal for the organic experiments were expressed by $\Delta(C_2H_4O_2^+/\text{organic})$. No corrections for water content were made given the lower hygroscopicity of organic material compared to ammonium sulfate[44] as well as the uncertainty in uptake for different mass concentrations of the organic particles.[45] In the presence of gas-phase levoglucosan, at 10% RH the value of $\Delta(C_2H_4O_2^+/\text{organic})$ increased by $(2.7 \pm 0.8) \times 10^{-4}$ relative to the background signal (Figure 3f and Table 1). It further increased to $(4.6 \pm 0.9) \times 10^{-4}$ at 40% RH. Above 40% RH, uptake did not increase further, at least within experimental uncertainty (i.e., $\Delta(C_2H_4O_2^+/\text{organic}) = (5.1 \pm 0.8) \times 10^{-4}$ for >95% RH). A comparison of Figure 3b and f shows that $\Delta(C_2H_4O_2^+/\text{organic})$ did not depend on whether RH was increased or decreased. The plot of $\Delta(C_6H_7^+/\text{organic})$ is discussed further in Section 3.4 as a control experiment.

3.3. No Observable Uptake of 2,4-Dinitrophenol by α-Pinene-Derived Organic Particles. The results of 2,4-dinitrophenol uptake by α-pinene-derived organic particles are presented in Figure 4 for 80% RH. The organic particle mass concentration (26.2 ± 0.7 μg m^{-3}) and the mass-equivalent concentration of the $\sum C_xH_yO_zN_w^+$ ion intensity from the AMS are plotted in Figure 4a and b, respectively. The ratio $\sum C_xH_yO_zN_w^+$/organic is plotted in Figure 4c. The electron-impact mass spectrum of 2,4-dinitrophenol suggests that the $\sum C_xH_yO_zN_w^+$ ion intensity accounted for 90% of the fractionation compared to 10% for NO^+ (m/z 30) and NO_2^+ (m/z 46).[46] The shaded area of Figure 4c represents the exposure period to gas-phase 2,4-dinitrophenol. As seen in Figure 4c, there was no difference within experimental uncertainty in the ratio $\sum C_xH_yO_zN_w^+$/organic for periods with and without exposure, indicating the absence of detectable 2,4-dinitrophenol uptake by the studied organic particles, at least for the conditions of the experiment. The uptake experiment was also conducted at 20% RH, and similar results were obtained.

The mass concentration of nitrogen-containing ions (i.e., $\sum C_xH_yO_zN_w^+$) was 0.07 ± 0.02 μg m^{-3} for both the exposure and nonexposure periods. This organic nitrogen content, representing (0.3 ± 0.1)% (w/w), might be related to the production of nitrogen-bearing compounds by contamination of 50 to 200 ppt NO_x in the zero air when producing the organic particles inside the HEC.[35]

3.4. Control Experiments. Several control experiments were conducted to verify that positive values of $\Delta(C_2H_4O_2^+/\text{ammonium sulfate})$ and $\Delta(C_2H_4O_2^+/\text{organic})$ represented uptake. In the ammonium sulfate experiments, a filter, placed between the sulfate atomizer and the reaction flask to remove particles while continuing the flow of gas-phase levoglucosan into the flask, eliminated the AMS signal for $C_2H_4O_2^+$, indicating that the $C_2H_4O_2^+$ signal was due to levoglucosan uptake by sulfate particles rather than homogeneous nucleation of levoglucosan aerosol particles. For the experiments with organic particles, a filter placed between the HEC and the reaction flask eliminated the AMS signal for $C_2H_4O_2^+$, indicating that no gas-phase species interfered with the AMS PM measurement. Interrupting the flow of ozone into the HEC likewise eliminated the AMS signal for $C_2H_4O_2^+$. These two control experiments are consistent with levoglucosan uptake into organic particles as the explanation for positive values of $\Delta(C_2H_4O_2^+/\text{organic})$. As a check against drift with RH in the AMS analysis,[47] the quantity $(C_6H_7^+/\text{organic})$ is plotted in Figure 3e and f. The plot shows that $(C_6H_7^+/\text{organic})$ was not influenced by changes in RH. It was also not

DOI: 10.1021/acs.est.8b02119
Environ. Sci. Technol. 2018, 52, 8381−8389

influenced by exposure to levoglucosan. The $C_6H_7^+$ ion was chosen for control analyses because the organic particles contribute to its signal strength but levoglucosan does not. Other ions (e.g., $C_7H_7^+$, $C_5H_7O^+$, and $C_7H_9O^+$) that satisfied this same criterion also showed identical behavior (not shown). These results indicate that the AMS mass spectrum of the organic particles themselves was not influenced by RH.

4. DISCUSSION

Both kinetic and thermodynamic factors can regulate gas-particle interactions and ultimately molecular uptake. Thermodynamics, quantified by a gas-particle partitioning coefficient K, sets an upper limit of uptake. Partitioning theory describes the equilibrium between the particle-phase concentration of a species and its gas-phase concentration: $K = (C_p/M_p)/C_g$ for a species mass concentration C_p in the particle phase, a species mass concentration C_g in the gas phase, and a particle mass concentration M_p.[48] Units of K are $(\text{ng } \mu\text{g}^{-1})_{\text{particle}}/(\text{ng m}^{-3})_{\text{gas}}$. For a sufficiently long exposure time τ_{equi} to a gas-phase species, equilibrium is achieved, and uptake saturates at the thermodynamic limit of the partitioning coefficient. Kinetics determines the rate at which uptake occurs, regulating the value of τ_{equi}. Kinetic effects are observed and uptake is kinetically limited in the case that an experiment has a characteristic time τ_{exp} that is less than τ_{equi}. For some scenarios, species diffusivity in the particle, which depends on particle physical state, can have a dominant role in determining τ_{equi} of uptake. As an example, the rate of uptake is expected to be significantly suppressed on a solid or semisolid particle, which has low diffusivity, as compared to a liquid particle, thus significantly increasing τ_{equi}.[49] Herein, the data sets are discussed in the paradigm of thermodynamic and kinetic factors.

4.1. Uptake of Levoglucosan by Ammonium Sulfate Particles. The sulfate experiments provide an example of uptake in the thermodynamic regime. For submicron aqueous particles, molecular diffusion of levoglucosan for full mixing throughout the particle should correspond to $\tau_{\text{equi}} < 1$ s,[13] which is far less than τ_{exp} of 200 s. As a result, the amount of uptake was considered as an equilibrium condition described by K. Based on dry ammonium sulfate mass concentration, its value increased from $(1.2 \pm 0.1) \times 10^{-3}$ $(\text{ng } \mu\text{g}^{-1})/(\text{ng m}^{-3})$ at 40% RH, to $(1.5 \pm 0.1) \times 10^{-3}$ at 60% RH, to $(1.8 \pm 0.1) \times 10^{-3}$ at 80% RH, and to $(2.1 \pm 0.1) \times 10^{-3}$ for >95% RH, respectively (blue points, Figure 5a) (SI, Section S3). When incorporating water content, the K value decreased from $(1.0 \pm 0.1) \times 10^{-3}$ $(\text{ng } \mu\text{g}^{-1})/(\text{ng m}^{-3})$ at 40% RH, to $(0.9 \pm 0.1) \times 10^{-3}$ at 60% RH, to $(0.7 \pm 0.1) \times 10^{-3}$ at 80% RH, and to $(0.2 \pm 0.1) \times 10^{-3}$ for >95% RH, respectively (cyan points, Figure 5a) (SI, Section S2). The explanation for the dependence of K on RH is that the particle water content decreased in tandem with decreasing RH, leading to more concentrated solutions of ammonium sulfate and suggesting a salting-in effect for the interactions between levoglucosan and ionic ammonium sulfate.[50] Similar results were reported for glyoxal in aqueous ammonium sulfate, for which increased glyoxal uptake was explained by sulfate-enhanced hydration of glyoxal.[51] By comparison, the absorptive gas-particle partitioning coefficient for solid ammonium sulfate particles at 10%, 20%, and 60% RH was effectively zero, and uptake was limited to surface adsorption (red points, Figure 5a). The comparative results at 60% RH also highlight that across the RH range of the hysteresis loop from 35% to 80% RH, in which sulfate particles can be either aqueous or solid based on the RH history, the uptake of levoglucosan was favored for aqueous particles along the upper side of the hysteresis loop compared to solid particles along the lower side.

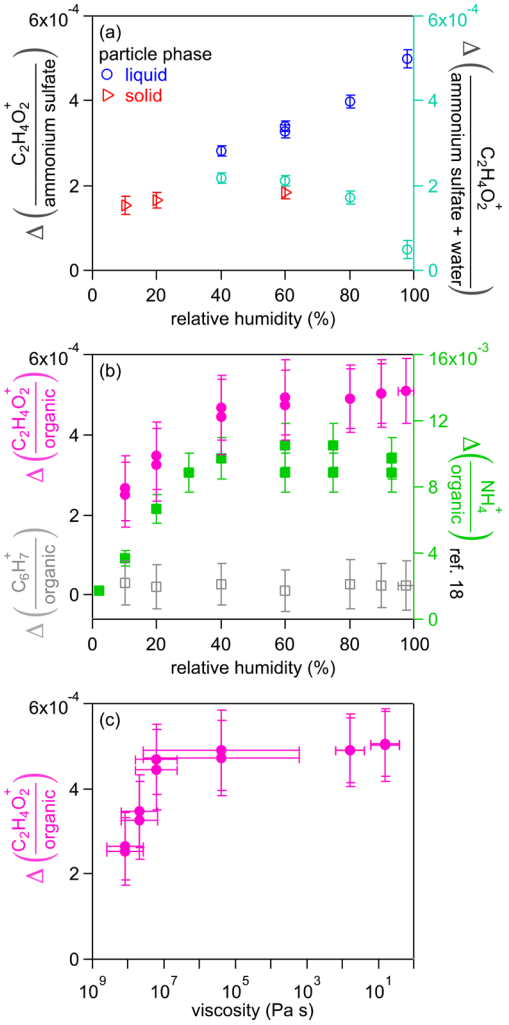

Figure 5. Summarized results for levoglucosan uptake, represented by the $C_2H_4O_2^+$ ion. (a) Ammonium sulfate particles and (b) α-pinene-derived organic PM. For ammonium sulfate, uptake is normalized to ammonium sulfate on the left axis and to (ammonium sulfate + water) on the right axis (SI, Section S3). For organic particles, results are also shown for a control ion ($C_6H_7^+$), which was a strong ion for α-pinene-derived organic PM and to which levoglucosan did not contribute (this study), as well as for ammonia uptake, as reported by Li et al.[18] in similar experiments. (c) Relationship between levoglucosan uptake and the viscosity of α-pinene-derived organic material. Viscosity values are taken from Zhang et al. and Renbaum-Wolff et al.[56,62]

4.2. Uptake of Levoglucosan and 2,4-Dinitrophenol by Organic Particles. *4.2.1. Thermodynamic Regime.* For the experiments using α-pinene-derived organic particles, levoglucosan uptake saturated above 40% RH (Figure 5b). An earlier study of ammonia uptake by α-pinene-derived organic particles also observed 40% RH as a critical RH for cross over into a saturation regime (also plotted in Figure 5b).[18] The explanation was that the mixing time for diffusion throughout the particles was on the same order of the experimental exposure time. The implication was a shift at 40% RH from a kinetic regime to a thermodynamic one that was limited by the gas-particle partitioning coefficient for 40% to

DOI: 10.1021/acs.est.8b02119
Environ. Sci. Technol. 2018, 52, 8381−8389

>95% RH. Total ammonia uptake in that study was 20 times greater than that of levoglucosan in this study, possibly due to the high concentration of gas-phase ammonia (5 ppm) as well as a component of reactive uptake associated with the production of organo-nitrogen compounds within the particle.[18] This study and that of ref 18 were carried out for highly different chemical uptake species yet otherwise similar in terms of similarly sized populations of α-pinene-derived organic particles produced by similar chemical methods. Both studies point to the shift from a kinetic to a thermodynamic regime at 40% RH for uptake, whether for levoglucosan or ammonia. The dominant factor influencing this shift can be attributed to the commonality of the change in viscosity of the organic particles and hence the diffusivity of the uptake species.

The experimentally observed uptake of levoglucosan was $(2.6 \pm 0.6) \times 10^{-2}$ $\mu g\ m^{-3}$ at 40% RH based on the AMS fraction of $C_2H_4O_2^+$ ion in levoglucosan, the observed ratio $\Delta(C_2H_4O_2^+/organic)$, and the mass concentration of organic particles. This amount of uptake corresponded to $K = (2.0 \pm 0.4) \times 10^{-3}$ $(ng\ \mu g^{-1})/(ng\ m^{-3})$ (SI, Section S3). The possible upward trend for ratio $\Delta(C_2H_4O_2^+/organic)$ suggested in Figure 5b above 40% RH, yet within the uncertainty bars, could be explained by the small yet increasing water content with RH, which was not included in the analysis because of discussed uncertainties.

The observed uptake and the corresponding partitioning coefficient can be compared to estimated values. The gas-particle partitioning coefficient was estimated as follows: $K = MW(\overline{MW}C_g^0\gamma)^{-1}$ where MW is the molecular weight of the gas-phase species, $\overline{MW}$ is the average molecular weight of the particle-phase material, C_g^0 is the mass concentration of the gas over the pure liquid compound of the absorbing species, and γ is its activity coefficient. Quantity C_g^0 was estimated by group contribution methods (SI, Section S4).[52] Quantity γ was estimated through Hansen solubility parameters that are commonly used to predict intermolecular interactions between organic compounds.[53,54] The estimated K value was $(3.5 \pm 2.7) \times 10^{-3}$ $(ng\ \mu g^{-1})/(ng\ m^{-3})$ compared to the measured value of $(2.0 \pm 0.4) \times 10^{-3}$ $(ng\ \mu g^{-1})/(ng\ m^{-3})$. The corresponding estimated uptake C_p was $(4.6 \pm 3.6) \times 10^{-2}$ $\mu g\ m^{-3}$ compared to the observation of $(2.6 \pm 0.6) \times 10^{-2}$ $\mu g\ m^{-3}$.

The uptake of 2,4-dinitrophenol was negligible within experimental uncertainty. The expected uptake, following a similar analysis to that presented above for levoglucosan, was $(7.8 \pm 6.2) \times 10^{-2}$ $\mu g\ m^{-3}$. For comparison, the experimental detection limit for the $\sum C_xH_yO_zN_w^+$ family was 12×10^{-2} $\mu g\ m^{-3}$ or higher.[38] Based on this detection limit and the expected uptake, the apparent absence of uptake in the experiments is justified. Correspondingly, $K < 6.8 \times 10^{-6}$ $(ng\ \mu g^{-1})/(ng\ m^{-3})$ is required to explain the apparent absence of uptake. This upper limit can be compared to 0.21×10^{-6} $(ng\ \mu g^{-1})/(ng\ m^{-3})$, which corresponds to the Henry's law constant for 2,4-dinitrophenol in water.[55] Compared to levoglucosan, 2,4-dinitrophenol shows a much higher mass concentration of the gas over the pure liquid compound, which justifies the lower gas-particle partitioning coefficient of 2,4-dinitrophenol (SI, Section S4).

4.2.2. Kinetic Regime. The experiments on levoglucosan uptake on the organic particles from 10% to 40% RH provide an example of the transition of uptake from a kinetic to a thermodynamic regime. For α-pinene-derived organic PM, the particles established equilibrium with surrounding RH in <1 s across this RH range,[13] and the viscosity changed in a smooth transition by a factor of 10 (Table 1). Diffusivity of water is faster than that of larger molecules.[19] Levoglucosan uptake tracked the gradual transition in physical state (Figure 5c). The diffusivity for levoglucosan in the organic matrix can be estimated as $10^{-19\pm0.05}$ $m^2\ s^{-1}$ at 40% RH based on the Stokes–Einstein relation and an equivalent molecular radius of 0.34 nm (SI, Section S5).[6,12,56] The Stokes–Einstein relation was tested[19] and holds for estimating the diffusivity of medium-sized molecules that have similar sizes to the molecules of the organic matrix where the organic particles are not in a glassy state. This diffusivity would correspond to 10^3 s for full mixing of organic molecules within a 100 nm particle at 40% RH.[56] By comparison, a similar analysis for viscosities at 30% and 50% RH would suggest 2×10^3 s and 10^2 s, respectively, for full mixing. The estimated time scale of 10^3 s at 40% RH is on the same order of the experimental time scale of 200 s in the reaction flask, thus supporting the interpretation of a transition from a kinetic to a thermodynamic regime at this RH.

In summary, the results herein show that the uptake of medium-sized organic molecules on atmospherically relevant organic and inorganic particles can be regulated by both kinetic and thermodynamic factors, represented by molecular diffusivities and gas-particle partitioning coefficients, respectively. Some atmospheric models treat uptake through an assumption that molecular diffusivity inside particles is high enough that the particle composition remains well mixed at all times.[57−59] This assumption corresponds to the thermodynamic limit. Even when significant uptake is thermodynamically favorable, however, kinetic factors can limit the observed uptake during a fixed observation period.[15,18] The results herein highlight the importance of relative humidity in the transition from a kinetically limited regime at low RH to a thermodynamically limited one at high RH. The prevailing regime, regulated by the particle physical state, can greatly influence multiphase chemical reactions[18] and thus the evolution of particle properties, such as refractive index[19] or cloud- and ice-nucleating activities.[60,61]

■ ASSOCIATED CONTENT

Supporting Information

The Supporting Information is available free of charge on the ACS Publications website at DOI: 10.1021/acs.est.8b02119.

One figure with additional experimental results, and calculation details with two supplementary tables (PDF)

■ AUTHOR INFORMATION

Corresponding Author

*E-mail: scot_martin@harvard.edu.

ORCID

Zhaoheng Gong: 0000-0002-9451-2060
Pengfei Liu: 0000-0001-7280-9720
Jianhuai Ye: 0000-0002-9063-3260
Karena A. McKinney: 0000-0003-1129-1678

Present Address

‖Colby College, Department of Chemistry, Waterville, Maine 04901, United States.

Notes

The authors declare no competing financial interest.

DOI: 10.1021/acs.est.8b02119
Environ. Sci. Technol. 2018, 52, 8381−8389

■ ACKNOWLEDGMENTS

This research was funded by the Atmospheric System Research Program of the Office of Science of the Department of Energy (DE-SC0012792) and by the Geosciences Directorate of the National Science Foundation (AGS-1249565). We acknowledge Suzane de Sá for fruitful discussion.

■ REFERENCES

(1) IPCC, 2013: Climate Change 2013: The Physical Science Basis. *Contribution of Working Group I to the Fifth Assessment Report of the Intergovernmental Panel on Climate Change*; Stocker, T. F.; Qin, D.; Plattner, G. -K.; Tignor, M.; Allen, S. K.; Boschung, J.; Nauels, A.; Xia, Y.; Bex, V.; Midgley, P. M., Eds.; Cambridge University Press: Cambridge, United Kingdom and New York, NY, 2013; http://www.climatechange2013.org/report/full-report/.

(2) Di, Q.; Wang, Y.; Zanobetti, A.; Wang, Y.; Koutrakis, P.; Choirat, C.; Dominici, F.; Schwartz, J. D. Air Pollution and Mortality in the Medicare Population. *N. Engl. J. Med.* **2017**, *376*, 2513−2522.

(3) Martin, S. T. Phase transitions of aqueous atmospheric particles. *Chem. Rev.* **2000**, *100*, 3403−3453.

(4) Virtanen, A.; Joutsensaari, J.; Koop, T.; Kannosto, J.; Yli-Pirila, P.; Leskinen, J.; Makela, J. M.; Holopainen, J. K.; Poschl, U.; Kulmala, M.; Worsnop, D. R.; Laaksonen, A. An amorphous solid state of biogenic secondary organic aerosol particles. *Nature* **2010**, *467*, 824−827.

(5) Abbatt, J. P.; Lee, A. K.; Thornton, J. A. Quantifying trace gas uptake to tropospheric aerosol: recent advances and remaining challenges. *Chem. Soc. Rev.* **2012**, *41*, 6555−6581.

(6) Koop, T.; Bookhold, J.; Shiraiwa, M.; Pöschl, U. Glass transition and phase state of organic compounds: dependency on molecular properties and implications for secondary organic aerosols in the atmosphere. *Phys. Chem. Chem. Phys.* **2011**, *13*, 19238−19255.

(7) Krieger, U. K.; Marcolli, C.; Reid, J. P. Exploring the complexity of aerosol particle properties and processes using single particle techniques. *Chem. Soc. Rev.* **2012**, *41*, 6631−6662.

(8) Ziemann, P. J.; Atkinson, R. Kinetics, products, and mechanisms of secondary organic aerosol formation. *Chem. Soc. Rev.* **2012**, *41*, 6582−6605.

(9) Zobrist, B.; Marcolli, C.; Pedernera, D. A.; Koop, T. Do atmospheric aerosols form glasses? *Atmos. Chem. Phys.* **2008**, *8*, 5221−5244.

(10) Mikhailov, E.; Vlasenko, S.; Martin, S. T.; Koop, T.; Schl, U. P. Amorphous and crystalline aerosol particles interacting with water vapor: conceptual framework and experimental evidence for restructuring, phase transitions and kinetic limitations. *Atmos. Chem. Phys.* **2009**, *9*, 9491−9522.

(11) Bateman, A. P.; Gong, Z.; Liu, P.; Sato, B.; Cirino, G.; Zhang, Y.; Artaxo, P.; Bertram, A. K.; Manzi, A. O.; Rizzo, L. V.; Souza, R. A. F.; Zaveri, R. A.; Martin, S. T. Sub-micrometre particulate matter is primarily in liquid form over Amazon rainforest. *Nat. Geosci.* **2016**, *9*, 34−37.

(12) Bones, D. L.; Reid', J. P.; Lienhard, D. M.; Krieger, U. K. Comparing the mechanism of water condensation and evaporation in glassy aerosol. *Proc. Natl. Acad. Sci. U. S. A.* **2012**, *29*, 11613−11618.

(13) Liu, P.; Li, Y. J.; Wang, Y.; Gilles, M. K.; Zaveri, R. A.; Bertram, A. K.; Martin, S. T. Lability of secondary organic particulate matter. *Proc. Natl. Acad. Sci. U. S. A.* **2016**, *113*, 12643−12648.

(14) Mendez, M.; Visez, N.; Gosselin, S.; Crenn, V.; Riffault, V.; Petitprez, D. Reactive and nonreactive ozone uptake during aging of oleic acid particles. *J. Phys. Chem. A* **2014**, *118*, 9471−9481.

(15) F.McNeill, V.; Patterson, J.; M.Wolfe, G.; Thornton, J. A. The effect of varying levels of surfactant on the reactive uptake of N_2O_5 to aqueous aerosol. *Atmos. Chem. Phys.* **2006**, *6*, 1635−1644.

(16) Lakey, P. S. J.; Berkemeier, T.; Krapf, M.; Dommen, J.; Steimer, S. S.; Whalley, L. K.; Ingham, T.; Baeza-Romero, M. T.; Pöschl, U.; Shiraiwa, M.; Ammann, M.; Heard, D. E. The effect of viscosity and diffusion on the HO_2 uptake by sucrose and secondary organic aerosol particles. *Atmos. Chem. Phys.* **2016**, *16*, 13035−13047.

(17) Kuwata, M.; Martin, S. T. Phase of atmospheric secondary organic material affects its reactivity. *Proc. Natl. Acad. Sci. U. S. A.* **2012**, *109*, 17354−17359.

(18) Li, Y. J.; Liu, P.; Gong, Z.; Wang, Y.; Bateman, A. P.; Bergoend, C.; Bertram, A. K.; Martin, S. T. Chemical reactivity and liquid/nonliquid states of secondary organic material. *Environ. Sci. Technol.* **2015**, *49*, 13264−13274.

(19) Liu, P.; Li, Y. J.; Wang, Y.; Bateman, A. P.; Zhang, Y.; Gong, Z.; Bertram, A. K.; Martin, S. T. Highly viscous states affect the browning of atmospheric organic particulate matter. *ACS Cent. Sci.* **2018**, *4*, 207−215.

(20) Kuwata, M.; Liu, Y.; McKinney, K.; Martin, S. T. Physical state and acidity of inorganic sulfate can regulate the production of secondary organic material from isoprene photooxidation products. *Phys. Chem. Chem. Phys.* **2015**, *17*, 5670−5678.

(21) Liu, Y.; Kuwata, M.; Strick, B. F.; Geiger, F. M.; Thomson, R. J.; McKinney, K. A.; Martin, S. T. Uptake of epoxydiol isomers accounts for half of the particle-phase material produced from isoprene photooxidation via the HO2 pathway. *Environ. Sci. Technol.* **2015**, *49*, 250−258.

(22) Zhang, Y.; Chen, Y.; Lambe, A. T.; Olson, N. E.; Lei, Z.; Craig, R. L.; Zhang, Z.; Gold, A.; Onasch, T. B.; Jayne, J. T.; Worsnop, D. R.; Gaston, C. J.; Thornton, J. A.; Vizuete, W.; Ault, A. P.; Surratt, J. D. Effect of the Aerosol-Phase State on Secondary Organic Aerosol Formation from the Reactive Uptake of Isoprene-Derived Epoxydiols (IEPOX). *Environ. Sci. Technol. Lett.* **2018**, *5*, 167−174.

(23) Shiraiwa, M.; Ammann, M.; Koop, T.; Pöschl, U. Gas uptake and chemical aging of semisolid organic aerosol particles. *Proc. Natl. Acad. Sci. U. S. A.* **2011**, *108*, 11003−11008.

(24) Hawthorne, S. B.; Miller, D. J.; Langenfeld, J. J.; Krlegsrt, M. S. PM-10 high-volume collection and quantitation of semi- and nonvolatile phenols, methoxylated phenols, alkanes, and polycyclic aromatic hydrocarbons from winter urban air and their relationship to wood smoke emissions. *Environ. Sci. Technol.* **1992**, *26*, 2251−2262.

(25) Simoneit, B. R. T.; Schauer, J. J.; Nolte, C. G.; Oros, D. R.; Elias, V. O.; Fraser, M. P.; Rogge, W. F.; Cass, G. R. Levoglucosan, a tracer for cellulose in biomass burning and atmospheric particles. *Atmos. Environ.* **1999**, *33*, 173−182.

(26) Zarzana, K. J.; Haan, D. O. D.; Freedman, M. A.; Hasenkop, C. A.; Tolbert, M. A. Optical properties of the products of α-dicarbonyl and amine reactions in simulated cloud droplets. *Environ. Sci. Technol.* **2012**, *46*, 4845−4851.

(27) May, A. A.; Lee, T.; McMeeking, G. R.; Akagi, S.; Sullivan, A. P.; Urbanski, S.; Yokelson, R. J.; Kreidenweis, S. M. Observations and analysis of organic aerosol evolution in some prescribed fire smoke plumes. *Atmos. Chem. Phys.* **2015**, *15*, 6323−6335.

(28) Tkacik, D. S.; Robinson, E. S.; Ahern, A.; Saleh, R.; Stockwell, C.; Veres, P.; Simpson, I. J.; Meinardi, S.; Blake, D. R.; Yokelson, R. J.; Presto, A. A.; Sullivan, R. C.; Donahue, N. M.; Robinson, A. L. A dual-chamber method for quantifying the effects of atmospheric perturbations on secondary organic aerosol formation from biomass burning emissions. *J. Geophys. Res. Atmos.* **2017**, *122*, 6043−6058.

(29) Jayne, J. T.; Leard, D. C.; Zhang, X.; Davidovits, P.; Smith, K. A.; Kolb, C. E.; R.Worsnop, D. Development of an aerosol mass spectrometer for size and composition analysis of submicron particles. *Aerosol Sci. Technol.* **2000**, *33*, 49−70.

(30) Ye, Q.; Upshur, M. A.; Robinson, E. S.; Geiger, F. M.; Sullivan, R. C.; Thomson, R. J.; Donahue, N. M. Following Particle-Particle Mixing in Atmospheric Secondary Organic Aerosols by Using Isotopically Labeled Terpenes. *Chem.* **2018**, *4*, 318−333.

(31) Jimenez, J. L.; Canagaratna, M. R.; Donahue, N. M.; Prevot, A. S.; Zhang, Q.; Kroll, J. H.; Decarlo, P. F.; Allan, J. D.; Coe, H.; Ng, N. L. Evolution of organic aerosols in the atmosphere. *Science* **2009**, *326*, 1525−1529.

(32) Guenther, A. B.; Jiang, X.; Heald, C. L.; Sakulyanontvittaya, T.; Duhl, T.; Emmons, L. K.; Wang, X. The model of emissions of gases and aerosols from nature version 2.1 (MEGAN2.1): an extended and updated framework for modeling biogenic emissions. *Geosci. Model Dev.* **2012**, *5*, 1471−1492.

DOI: 10.1021/acs.est.8b02119
Environ. Sci. Technol. 2018, 52, 8381−8389

(33) Gao, Y.; Chen, S. B.; Yu, L. E. Efflorescence relative humidity for ammonium sulfate particles. *J. Phys. Chem. A* **2006**, *110*, 7602−7608.
(34) Shilling, J. E.; Chen, Q.; King, S. M.; Rosenoern, T.; Kroll, J. H.; R.Worsnop, D.; McKinney, K. A.; Martin, S. T. Particle mass yield in secondary organic aerosol formed by the dark ozonolysis of α-pinene. *Atmos. Chem. Phys.* **2008**, *8*, 2073−2088.
(35) Liu, Y. J.; Herdlinger-Blatt, I.; McKinney, K. A.; Martin, S. T. Production of methyl vinyl ketone and methacrolein via the hydroperoxyl pathway of isoprene oxidation. *Atmos. Chem. Phys.* **2013**, *13*, 5715−5730.
(36) Booth, A. M.; Montague, W. J.; Barley, M. H.; Topping, D. O.; McFiggans, G.; Garforth, A.; Percival, C. J. Solid state and sub-cooled liquid vapour pressures of cyclic aliphatic dicarboxylic acids. *Atmos. Chem. Phys.* **2011**, *11*, 655−665.
(37) Schwarrenbach, R. P.; Stierli, R.; Folsom, B. R.; Zeyer, J. Compound properties relevant for assessing the environmental partitioning of nitrophenols. *Environ. Sci. Technol.* **1988**, *22*, 83−92.
(38) Chen, Q.; Liu, Y.; Donahue, N. M.; Shilling, J. E.; Martin, S. T. Particle-phase chemistry of secondary organic material: modeled compared to measured O: C and H: C elemental ratios provide constraints. *Environ. Sci. Technol.* **2011**, *45*, 4763−4770.
(39) Alfarra, M. R.; Coe, H.; Allan, J. D.; Bower, K. N.; Boudries, H.; Canagaratna, M. R.; Jimenez, J. L.; Jayne, J. T.; Garforth, A. A.; Li, S.-M.; Worsnop, D. R. Characterization of urban and rural organic particulate in the Lower Fraser Valley using two Aerodyne Aerosol Mass Spectrometers. *Atmos. Environ.* **2004**, *38*, 5745−5758.
(40) Cubison, M. J.; Ortega, A. M.; Hayes, P. L.; Farmer, D. K.; Day, D.; Lechner, M. J.; Brune, W. H.; Apel, E.; Diskin, G. S.; Fisher, J. A.; Fuelberg, H. E.; Hecobian, A.; Knapp, D. J.; Mikoviny, T.; Riemer, D.; Sachse, G. W.; Sessions, W.; Weber, R. J.; Weinheimer, A. J.; Wisthaler, A.; Jimenez, J. L. Effects of aging on organic aerosol from open biomass burning smoke in aircraft and laboratory studies. *Atmos. Chem. Phys.* **2011**, *11*, 12049−12064.
(41) Schneider, J.; Weimer, S.; Drewnick, F.; Borrmann, S.; Helas, G.; Gwaze, P.; Schmid, O.; Andreae, M. O.; Kirchner, U. Mass spectrometric analysis and aerodynamic properties of various types of combustion-related aerosol particles. *Int. J. Mass Spectrom.* **2006**, *258*, 37−49.
(42) Aiken, A. C.; DeCarlo, P. F.; Jimene, J. L. Elemental Analysis of Organic Species with Electron Ionization High-Resolution Mass Spectrometry. *Anal. Chem.* **2007**, *79*, 8350−8358.
(43) Allan, J. D.; Delia, A. E.; Coe, H.; Bower, K. N.; Alfarra, M. R.; Jimenez, J. L.; Middlebrook, A. M.; Drewnick, F.; Onasch, T. B.; Canagaratna, M. R.; Jayne, J. T.; Worsnop, D. R. A generalised method for the extraction of chemically resolved mass spectra from Aerodyne aerosol mass spectrometer data. *J. Aerosol Sci.* **2004**, *35*, 909−922.
(44) Varutbangkul, V.; Brechtel, F. J.; Bahreini, R.; Ng, N. L.; Keywood, M. D.; Kroll, J. H.; Flagan, R. C.; Seinfeld, J. H.; Lee, A.; Goldstein, A. H. Hygroscopicity of secondary organic aerosols formed by oxidation of cycloalkenes, monoterpenes, sesquiterpenes, and related compounds. *Atmos. Chem. Phys.* **2006**, *6*, 2367−2388.
(45) Smith, M. L.; Kuwata, M.; Martin, S. T. Secondary organic material produced by the dark ozonolysis of α-Pinene minimally affects the deliquescence and efflorescence of ammonium sulfate. *Aerosol Sci. Technol.* **2011**, *45*, 244−261.
(46) Mass spectrum (electron ionization) of 2,4-dinitrophenol; webbook.nist.gov/cgi/cbook.cgi?ID=C51285&Mask=200#Mass-Spec.
(47) Matthew, B. M.; Middlebrook, A. M.; Onasch, T. B. Collection efficiencies in an Aerodyne Aerosol Mass Spectrometer as a function of particle phase for laboratory generated aerosols. *Aerosol Sci. Technol.* **2008**, *42*, 884−898.
(48) Seinfeld, J. H.; Pankow, J. F. Organic atmospheric particulate material. *Annu. Rev. Phys. Chem.* **2003**, *54*, 121−140.
(49) Shiraiwa, M.; Zuend, A.; Bertram, A. K.; Seinfeld, J. H. Gas-particle partitioning of atmospheric aerosols: interplay of physical state, non-ideal mixing and morphology. *Phys. Chem. Chem. Phys.* **2013**, *15*, 11441−11453.
(50) You, Y.; Smith, M. L.; Song, M.; Martin, S. T.; Bertram, A. K. Liquid−liquid phase separation in atmospherically relevant particles consisting of organic species and inorganic salts. *Int. Rev. Phys. Chem.* **2014**, *33*, 43−77.
(51) Yu, G.; Bayer, A. R.; Galloway, M. M.; Korshavn, K. J.; Fry, C. G.; Keutsch, F. N. Glyoxal in aqueous ammonium sulfate solutions: products, kinetics and hydration effects. *Environ. Sci. Technol.* **2011**, *45*, 6336−6342.
(52) Pankow, J. F.; Asher, W. E. SIMPOL.1: a simple group contribution method for predicting vapor pressures and enthalpies of vaporization of multifunctional organic compounds. *Atmos. Chem. Phys.* **2008**, *8*, 2773−2796.
(53) Ye, J.; Gordon, C. A.; Chan, A. W. Enhancement in secondary organic aerosol formation in the presence of preexisting organic particle. *Environ. Sci. Technol.* **2016**, *50*, 3572−3579.
(54) Hansen, C. M. *Hansen Solubility Parameters: A User'S Handbook*, 2nd ed.; CRC Press: Boca Raton, 2007.
(55) Tremp, J.; Mattrel, P.; Fingler, S.; Giger, W. Phenols and nitrophenols as tropospheric pollutants: Emissions from automobile exhausts and phase transfer in the atmosphere. *Water, Air, Soil Pollut.* **1993**, *68*, 113−123.
(56) Renbaum-Wolff, L.; Grayson, J. W.; Bateman, A. P.; Kuwata, M.; Sellier, M.; Murray, B. J.; Shilling, J. E.; Martin, S. T.; Bertram, A. K. Viscosity of α-pinene secondary organic material and implications for particle growth and reactivity. *Proc. Natl. Acad. Sci. U. S. A.* **2013**, *110*, 8014−8019.
(57) Hanson, D. R. Surface-Specific Reactions on Liquids. *J. Phys. Chem. B* **1997**, *101*, 4998−5001.
(58) Schwartz, S. E.; Freiberg, J. E. Mass-transport limitation to the rate of reaction of gases in liquid droplets: Application to oxidation of SO2 in aqueous solutions. *Atmos. Environ.* **2007**, *15*, 1129−1144.
(59) Worsnop, D. R.; Morris, J. W.; Shi, Q.; Davidovits, P.; Kolb, C. E. A chemical kinetic model for reactive transformations of aerosol particles. *Geophys. Res. Lett.* **2002**, *29*, 57−1−57−4.
(60) Shilling, J. E.; King, S. M.; Mochida, M.; Worsnop, D. R.; Martin, S. T. Mass spectral evidence that small changes in composition caused by oxidative aging processes alter aerosol CCN properties. *J. Phys. Chem. A* **2007**, *111*, 3358−3368.
(61) Cziczo, D. J.; Froyd, K. D.; Gallavardin, S. J.; Moehler, O.; Benz, S.; Saathoff, H.; Murphy, D. M. Deactivation of ice nuclei due to atmospherically relevant surface coatings. *Environ. Res. Lett.* **2009**, *4*, 044013.
(62) Zhang, Y.; Sanchez, M. S.; Douet, C.; Wang, Y.; Bateman, A. P.; Gong, Z.; Kuwata, M.; Renbaum-Wolff, L.; Sato, B. B.; Liu, P. F.; Bertram, A. K.; Geiger, F. M.; Martin, S. T. Changing shapes and implied viscosities of suspended submicron particles. *Atmos. Chem. Phys.* **2015**, *15*, 7819−7829.

DOI: 10.1021/acs.est.8b02119
Environ. Sci. Technol. 2018, 52, 8381−8389